JOURNAL OF AGRICULTURAL AND FOOD CHEMISTRY

Tyrosinase Inhibitory Polyphenols from Roots of *Morus lhou*

SEONG HUN JEONG,[†,‡] YOUNG BAE RYU,[†,‡] MARCUS J. CURTIS-LONG,[§] HYUNG WON RYU,[†] YOON SU BAEK,[†] JAE EUN KANG,[†] WOO SONG LEE,[||] AND KI HUN PARK*[,†]

Division of Applied Life Science (BK21 Program), EB-NCRC, Institute of Agriculture & Life Science, Graduate School of Gyeongsang National University, Jinju 660-701, Korea, 12 New Road, Nafferton, Driffield, East Yorkshire YO25 4JP, U.K., and Bioindustry Research Center, Korea Research Institute of Bioscience and Biotechnology, Jeoungeup 580-185, Korea

Twelve polyphenols (**1**−**12**) possessing tyrosinase inhibitory properties were isolated from the methanol (95%) extract of *Morus lhou*. The isolated compounds consisted of four flavanones (**1**−**4**), four flavones (**5**−**8**), and four phenylbenzofuranes (**9**−**12**). Moracin derivative **12** proved to be new a compound which was fully characterized. Compounds **1**−**12** were evaluated for both monophenolase and diphenolase (the two steps catalyzed by tyrosinase) inhibition to identify the structural characteristics required for mushroom tyrosinase inhibition. We observed that all parent compounds (**1**, **5**, and **9**) possessing an unsubstituted resorcinol group were highly effective inhibitors of monophenolase activity (IC_{50} values of 1.3, 1.2, and 7.4 μM). The potency of the inhibitors diminished with alkyl substitution on either the aromatic ring or the hydroxyl functions. Interestingly, flavone **5** was shown to possess only monophenolase inhibitory activity, but flavanone **1** and phenylbenzofuran **9** inhibited diphenolase as well as monophenolase significantly. The inhibitory mode of these species was also dependent upon the skeleton: phenylbenzofuran **9** manifested a simple competitive inhibition mode for monophenolase and diphenolase; on the other hand flavanone **1** (monophenolase, $k_3 = 0.1966$ min^{-1} μM^{-1}, $k_4 = 0.0082$ min^{-1}, and $K_i^{app} = 0.0468$ μM; diphenolase, $k_3 = 0.0014$ min^{-1} μM^{-1}, $k_4 = 0.0013$ min^{-1}, and $K_i^{app} = 0.8996$ μM) and flavone **5** both showed time-dependent inhibition against monophenolase. Compound **1** operated according to the simple reversible slow binding model whereas compound **5** operated under the enzyme isomerization model.

KEYWORDS: Tyrosinase; slow-binding; flavonoid; phenylbenzofuran; *Morus lhou*

INTRODUCTION

Tyrosinase (EC 1.14.18.1), also known as polyphenoloxidase (PPO), is an essential enzyme in numerous cellular processes including insect molting and the browning of damaged fruit. Its most well-known trait is the production of melanin for the protection of skin from UV radiation. However, overproduction of melanin results in skin hyperpigmentation, characterized by age spots, melasma and chloasma, all of which are common maladies (*1*−*3*). Thus control of melanin formation is directly linked to human disease prevention. In addition, the inhibition of melanin formation is also applicable to fruit preservation by the alleviation of browning. Tyrosinase is an enzyme containing binuclear copper. It catalyzes the conversion of tyrosine to 3,4-dihydroxy phenylalanine (DOPA), a process that is called monophenolase activity, and the oxidation of DOPA into DOPA quinine (diphenolase activity), which are the initial steps in the pathway (*4*−*6*). The highly reactive quinines spontaneously evolve through nonenzymatic coupling to brown pigments of high molecular weight. Tyrosinase inhibitors usually either chelate the copper ion within the tyrosinase active site, obstructing the substrate−enzyme interaction, or prevent oxidation via an electrochemical process (*7*−*9*).

Microorganisms and plants are the main sources of natural tyrosinase inhibitors. Hydroxylated flavonoids are good target compounds for tyrosinase inhibitors because they share structural similarities with L-tyrosine, the natural substrate for tyrosinase (*1*). *Morus lhou* (S.) Koidz. is well renowned as a polyphenol-rich plant that is one of the most ubiquitous traditional herbal medicines in East Asia. This species, belonging to the family of Moraceae, may be considered to be a nontoxic natural therapeutic agent. Its young leaves and twigs have been classified as edible by the KFDA (Korea Food & Drug Administration). Its main bioactive constituents are flavonoids,

* Corresponding author. Tel: +82-55-751-5472. Fax: +82-55-757-0178. E-mail: khpark@gsnu.ac.kr.
[†] Gyeongsang National University.
[‡] These authors contributed equally to this paper.
[§] 12 New Road, Nafferton, Driffield, East Yorkshire YO25 4JP, U.K.
[||] Korea Research Institute of Bioscience and Biotechnology.

10.1021/jf8033286 CCC: $40.75
Published on Web 01/23/2009

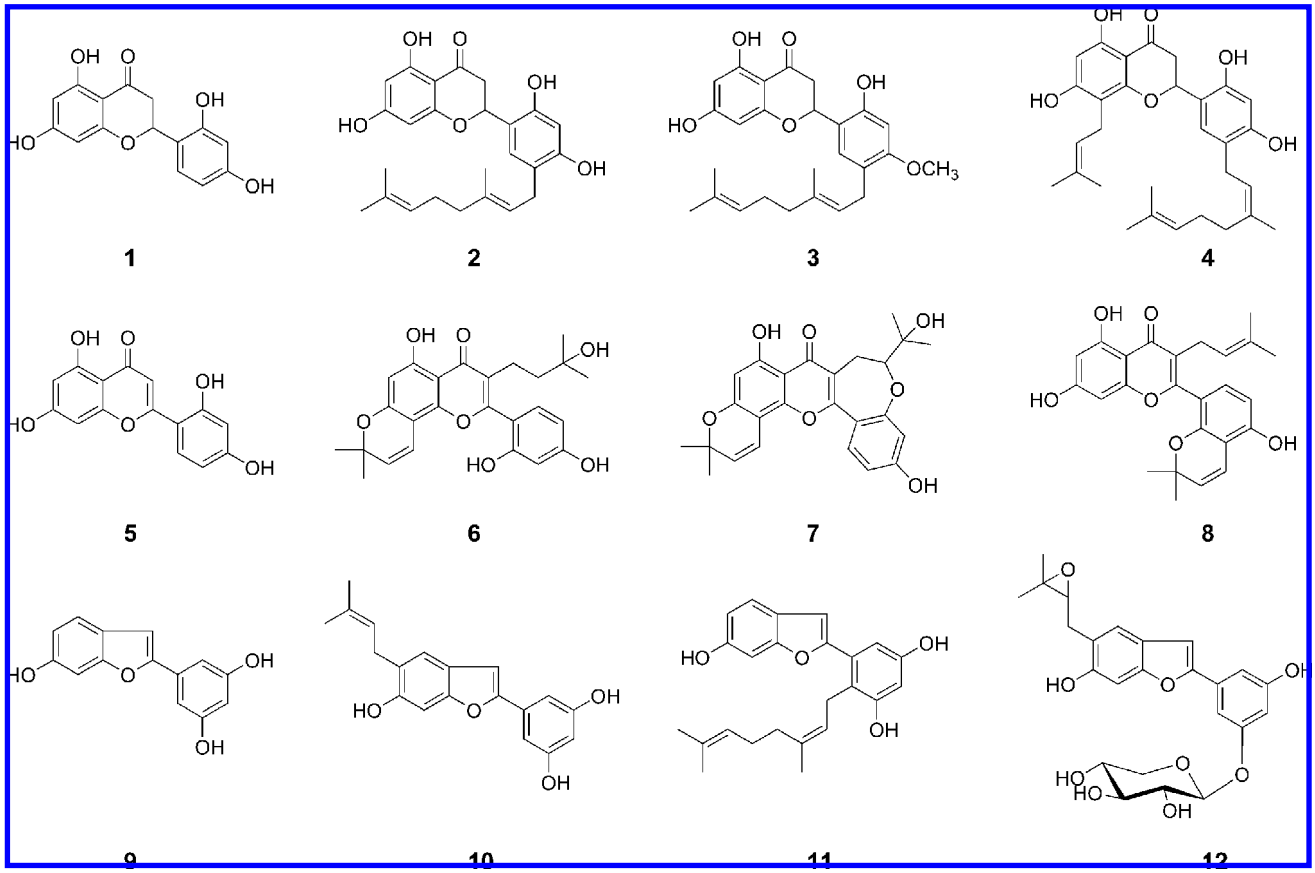

Figure 1. Chemical structures of isolated compounds **1**−**12** from the *M. lhou*.

cumarins, and terpenoids, many of which have been proven to have antibrowning (*10*, *11*), hypoglycemic (*12*), antinephritis (*13*), and anti-inflammatory properties (*14*). Previous workers reported that this species contains tyrosinase inhibiting flavanones, flavones, stilbenes and phenylbenzofurans. Extracts of this species, including stilbene derivatives, have been shown to be effective in the preservation of apple juice against browning (*15*). Mulberroside F showed an inhibitory effect on melanin formation within melanoma cells (*16*).

As melanin formation is a two-step process from tyrosine, its formation can be tempered by the inhibition of either stage. Although some reports have arisen regarding the tyrosinase inhibitory activities of Moraceae extracts, none of these have been able to disclose the detailed mechanism of enzyme activity with respect to the phenol. In this study, we isolated twelve flavonoids from the methanol extract of the roots of *M. lhou*, and identified their structures using spectroscopic methods (**Figure 1**).

MATERIALS AND METHODS

Plant Material. The roots of *Morus lhou* (S.) Koidz. (No-sang) were collected at Mt. Bi-Bong in Jinju, Korea, on April, 2006. This plant was identified by Gyeongsangnam-do Agricultural Research & Extension Services in Korea.

General Apparatus and Chemicals. Thin-layer chromatography (TLC) was carried out using commercially available glass plates precoated with silica gel (E. Merck Co., Darmstadt, Germany), and visualized under UV at 254 nm or stained with 10% H_2SO_4. Column chromatography was carried out using 230−400 mesh silica gel (Kieselgel 60, Merck, Germany). Melting points (mp) were measured on a Thomas Scientific capillary melting point apparatus (Electrothermal 9300, U.K.) and are uncorrected. UV spectra were measured on a Beckman DU650 spectrophotometer (Beckman Coulter, Fullerton, CA). ^{1}H and ^{13}C NMR data were all obtained on a Bruker AM 500 (^{1}H NMR at 500 MHz, ^{13}C NMR at 125 MHz) spectrometer (Bruker, Karlsruhe, Germany) in $CDCl_3$, acetone-d_6, DMSO-d_6, or methanol-d_4 with TMS as internal standard. EIMS was obtained on a JEOL JMS-700 mass spectrometer (JEOL, Tokyo, Japan). All reagent grade chemicals were purchased from Sigma Chemical Co. (St. Louis, MO).

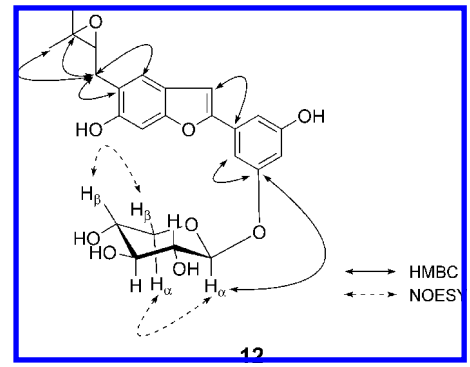

Figure 2. Selected correlations of HMBC and NOESY for compound **12**.

Extraction and Isolation. The roots of *M. lhou*(8 kg) were air-dried, chopped and extracted three times with methanol (15 L × 3, 95%) for 10 days at room temperature. The combined methanol extract was concentrated in vacuo to yield a dark brown gum (270 g). Vacuum liquid chromatography (VLC) of the methanol extract on celite was performed using an increasing gradient of $CHCl_3$ and MeOH. The $CHCl_3$ fraction (60 g) was chromatographed on silica gel (4 × 60 cm, 230−400 mesh, 400 g) using hexane/EtOAc [40:1 (0.4 L), 30:1 (0.4 L), 20:1 (0.4 L), 10:1 (0.4 L), 5:1 (0.4 L), 1:1 (1 L)] mixtures to furnish fractions A-E. Fraction D (15 g) was subjected to silica gel chromatography (3 × 60 cm) eluting with hexane/EtOAc (40:1 → 1:2) to give five fractions (fr. D.1−D.5); fr. D.1−D.2 were resubjected to silica gel chromatography with hexane/acetone (20:1 → 1:1) followed by column chromatography on Sephadex LH-20 [eluent: MeOH (2 × 90

Table 1. Tyrosinase inhibitory activity of isolated compounds (**1**−**12**)

	L-tyrosine		L-DOPA	
compound	IC_{50} (μM)[a]	type of inhibition (K_i, μM)[b]	IC_{50} (μM)	type of inhibition (K_i, μM)
1	1.3 ± 0.3	competitive (0.7 ± 0.1)	26.5 ± 2.2	competitive (14.1 ± 1.7)
2	47.5 ± 4.0	competitive (28.3 ± 1.5)	>200	NT[c]
3	>200	NT	>200	NT
4	44.2 ± 0.9	competitive (29.7 ± 1.0)	>200	NT
5	1.2 ± 0.4	competitive (0.61)	>200	NT
6	>200	NT	>200	NT
7	127.4 ± 3.9	competitive (78.3 ± 2.1)	>200	NT
8	131.8 ± 10.6	nt	>200	NT
9	7.4 ± 1.0	competitive (4.4 ± 1.6)	64.6 ± 2.2	competitive (39.0 ± 0.5)
10	160.3 ± 6.7	competitive (88.7 ± 3.9)	>200	NT
11	98.5 ± 0.7	NT	>200	NT
12	82.5 ± 1.2	competitive (33.4 ± 2.6)	>200	NT
kojic acid	16.3	NT	NT	NT

[a] All compounds were examined in a set of experiments repeated three times; IC_{50} values of compounds represent the concentration that caused 50% enzyme activity loss. [b] Values of inhibition constant. [c] Not tested.

cm)] to yield compound **4** (8 mg) and subsequently compound **8** (28 mg). Fr. E (18 g) was applied to a silica gel column (3 × 60 cm, 230−400 mesh, 170 g) [eluent: hexane/acetone (20:1 → 1:1)] to afford four subfractions fr. E.1−E.4. Fr. E.2−E.3 were resubjected to silica gel column {(4 × 70 cm, 230−400 mesh, 330 g) [eluent:hexane/EtOAc (60:1 → 1:2)]} to yield compounds **2** (135 mg) and **3**(54 mg). Further elution with hexane/Et_2O (30:1 → 1:4) generated compound **6** (12 mg). Mixture phase (110 g) was chromatographed on silica gel {(6 × 60 cm, 230−400 mesh, 800 g, eluent: $CHCl_3$/acetone [40:1 (1 L), 30:1 (1 L), 20:1 (1 L), 10:1 (1 L), 5:1 (1 L), 1:1 (3 L)]; followed by $CHCl_3$/MeOH [20:1 (1 L), 10:1 (1 L), 5:1 (1 L), 1:1 (3 L)]} to give fraction A−G. Fraction C (6 g) was subjected to silica gel column chromatography [eluent: $CHCl_3$/acetone (20:1 → 1:1)] followed by Sephadex LH-20 [eluent: MeOH (2 × 90 cm)] yielding **7** (18 mg). Fr. D (15 g) was applied to a silica gel column [3 × 60 cm, 230−400 mesh, 170 g, eluent: $CHCl_3$/MeOH (90:1 → 4:1)] to afford seven subfractions fr. D.1−D.7. Fr. D.3−D.5 were subjected to silica gel column [4 × 70 cm, 230−400 mesh, 330 g, eluent: $CHCl_3$/MeOH (60:1 → 2:1)] and then rechromatographed using octadecyl-functionalized silica gel (eluent: MeOH/H_2O 4/1) to yields compounds **1** (56 mg), **5** (17 mg) and **11** (25 mg). Fr. F (12 g) was chromatographed on silica gel [eluent: $CHCl_3$/MeOH (20:1 → 1:1)] to yield compound **9** (34 mg) and Sephadex LH-20 [eluent: MeOH (2 × 90 cm)] to give **10** (4 mg). Fr. G and MeOH phase were repeatedly chromatogaphed over silica gel using [eluent: $CHCl_3$/MeOH (20:1 → 1:1)] and then on Sephadex LH-20 [eluent: MeOH (2 × 90 cm)] to yield a new natural product, **12** (77 mg). All of the isolated compounds were identified on the basis of the following spectroscopic data (*10*, *17*−*23*).

Steppogenin (**1**)*:* colorless powder; mp 250−254 °C; $[\alpha]_D$ −3.5 (*c* 0.125, CH_3OH); HREIMS *m/z* 288.0642 (calcd for $C_{15}H_{12}O_6$, 288.0634); ^{1}H NMR (500 MHz, acetone-d_6) δ 7.18 (1H, d, J = 8.4 Hz, H-6′), 6.34 (1H, d, J = 2.3 Hz, H-3′), 6.30 (1H, dd, J = 8.4, 2.3 Hz, H-5′), 5.83 (1H, d, J = 2.0 Hz, H-6), 5.82 (1H, d, J = 2.1 Hz, H-8), 5.57 (1H, dd, J = 13.1, 2.9 Hz, H-2), 3.04 (1H, dd, J = 17.1, 13.1 Hz, H-3a), 2.69 (1H, dd, J = 17.1, 3.0 Hz, H-3b); ^{13}C NMR (125 MHz, acetone-d_6) δ 43.1 (C-3), 75.8 (C-2), 96.2 (C-8), 97.2 (C-6), 103.9 (C-3′, 4a), 105.3 (C-5′), 117.9 (C-1′), 129.4 (C-6′), 156.7 (C-2′), 159.9 (C-4′), 165.3 (C-8a), 166.1 (C-5), 167.8 (C-7), 198.1 (C-4).

Kuwanon E (**2**)*:* yellow powder; mp 121 °C; $[\alpha]_D$ −0.25 (*c* 0.291, CH_3OH); EIMS *m/z* (relative intensity) 424 (M^+, 22%), 406 (52%), 339 (19%), 301 (32%), 153 (100%); ^{1}H NMR (500 MHz, methanol-d_4) δ 7.09 (1H, s, H-6′), 6.37 (1H, s, H-3′), 5.92 (1H, J = 2.0 Hz, H-6), 5.90 (1H, J = 2.0 Hz, H-8), 5.62 (1H, dd, J = 12.6, 3.0 Hz, H-2), 5.31 (1H, m, H-2″), 5.12 (1H, m, H-7″), 3.23 (2H, d, J = 7.3 Hz, H-1″), 3.07 (1H, dd, J = 17.2, 12.6 Hz, H-3a), 2.72 (1H, dd, J = 17.1, 3.1 Hz, H-3b), 2.11 (2H, m, H-5″), 2.04 (2H, m, H-6″), 1.69 (3H, s, H-4″), 1.63 (3H, s, H-9″), 1.58 (3H, s, H-10″); ^{13}C NMR (125 MHz, methanol-d_4) δ 16.6 (C-4″), 18.2 (C-10″), 26.3 (C-9″), 28.2 (C-5″), 28.9 (C-1″), 41.3 (C-6″), 43.6 (C-3), 76.5 (C-2), 96.6 (C-8), 97.4 (C-6), 103.8 (C-3′), 103.8 (C-4a), 117.8 (C-1′), 121.1 (C-5′), 124.8 (C-2″), 125.9 (C-7″), 129.1 (C-6′), 132.6 (C-8″), 136.9 (C-3″), 154.9 (C-2′), 157.4 (C-4′), 165.8 (C-5), 165.9 (C-8a), 168.7 (C-7), 198.9 (C-4).

Kuwanon U (**3**)*:* amorphous yellow powder; mp 136−137 °C; $[\alpha]_D$ −2.4 (*c* 0.17, CH_3OH); EIMS *m/z* (relative intensity) 438 (M^+, 18%), 420 (29%), 315 (52%), 189 (49%), 153 (100%); ^{1}H NMR (500 MHz, $CDCl_3$) δ 6.86 (1H, s, H-6′), 6.37 (1H, s, H-3′), 5.94 (1H, s, H-6), 5.93 (1H, s, H-8), 5.51 (1H, dd, J = 12.8, 2.9 Hz, H-2), 5.18 (1H, m, H-2″), 5.03 (1H, m, H-7″), 3.73 (3H, s, OCH_3), 3.19 (2H, m, H-1″), 2.77−3.19 (2H, H-3), 2.02 (2H, m, H-5″), 1.974 (2H, m, H-6″), 1.60 (3H, s, H-4″), 1.58 (3H, s, H-9″), 1.51 (3H, s, H-10″); ^{13}C NMR (125 MHz, $CDCl_3$) δ 16.4 (C-4″), 18.1 (C-10″), 26.1 (C-9″), 27.2 (C-5″), 28.0 (C-1″), 40.2 (C-6″), 42.2 (C-3), 55.9 (C4′-OCH_3), 78.3 (C-2), 96.0 (C-8), 97.6 (C-6), 100.6 (C-3′), 103.7 (C-4a), 115.1 (C-1′), 122.6 (C-5′), 123.1 (C-2″), 124.7 (C-7″), 127.9 (C-6′), 131.8 (C-8″), 136.8 (C-3″), 153.7 (C-2′), 159.1 (C-4′), 162.9 (C-5), 164.8 (C-8a), 164.9 (C-7), 196.6 (C-4).

8-Isoprenyl-5′-geranyl-5,7,2′,4′-tetrahydroxy flavanone (**4**)*:* amorphous yellow powder; mp 161−165 °C; $[\alpha]_D$ −6.24 (*c* 0.158, CH_3OH); ^{1}H NMR (500 MHz, methanol-d_4) δ 7.03 (1H, s, H-6′), 6.25 (1H, s, H-3′), 5.82 (1H, s, H-6), 5.47 (1H, dd, J = 12.5, 3.0 Hz, H-2), 5.20 (1H, br t, H-2″), 5.08 (1H, m, H-10), 4.99 (1H, m, H-7″), 3.11 (2H, m, H-9), 3.08 (2H, m, H-1″), 2.65−2.84 (2H, m, H-3), 1.97 (2H, m, H-6″), 1.92 (2H, m, H-5″), 1.57 (3H, s, H-4″), 1.51 (3H, s, H-12), 1.50 (6H, s, H-9″, H-10″), 1.45 (3H, s, H-13); ^{13}C NMR (125 MHz, methanol-d_4) δ 16.7 (C-4″), 18.2 (C-9″), 18.5 (C-10″), 23.0 (C-9), 26.3 (C-12), 26.5 (C-13), 28.2 (C-6″), 28.9 (C-1″), 41.2 (C-5″), 43.7 (C-3), 76.4 (C-2), 96.7 (C-6), 103.8 (C-4a), 103.9 (C-3′), 109.5 (C-8), 118.3 (C-1′), 120.9 (C-5′), 124.4 C-10), 124.9 (C-2″), 125.9 (C-7″), 128.9 (C-6′), 131.9 (C-11), 132.5 (C-8″), 136.8 (C-3″), 154.6 (C-2′), 157.1 (C-4′), 162.5 (C-8a), 163.5 (C-5), 166.4 (C-7), 199.3 (C-4).

Norartocarpetin (**5**)*:* amorphous yellow powder; mp 330−340 °C; ^{1}H NMR (500 MHz, DMOS-d_6) δ 7.76 (1H, d, J = 8.8 Hz, H-6′), 6.99 (1H, s, H-3), 6.49 (1H, d, J = 2.3 Hz, H-3′), 6.44 (1H, m, H-5′), 6.43 (1H, d, J = 2.1 Hz, H-8), 6.17 (1H, d, J = 2.1 Hz, H-6); ^{13}C NMR (125 MHz, DMOS-d_6) δ 93.7 (C-8), 98.5 (C-6), 103.1 (C-4a), 103.4 (C-3′), 106.7 (C-3), 107.9 (C-5′), 108.5 (C-1′), 129.7 (C-6′), 157.2 (C-8a), 158.7 (C-2′), 161.3 (C-5), 161.7 (C-2), 161.7 (C-4′), 163.9 (C-7), 181.7 (C-4).

Morusinol (**6**)*:* amorphous yellow powder; mp 213−214 °C ^{1}H NMR (500 MHz, methanol-d_4) δ 7.04 (1H, d, J = 8.9 Hz, H-6′), 6.50 (1H, dd, J = 10.0, 0.5 Hz, H-9), 6.33 (2H, m, H-5′, H-3′), 5.49 (1H, d, J = 10.0 Hz, H-10), 2.36 (2H, m, H-1″), 1.50 (2H, m, H-2″), 1.34 (6H, s, H-12, H-13), 0.98 (6H, s, H-4″, H-5″); ^{13}C NMR (125 MHz, methanol-d_4) δ 16.7 (C-4″), 18.2 (C-9″), 18.5 (C-10″), 23.0 (C-9), 26.3 (C-12), 26.5 (C-13), 28.2 (C-6″), 28.9 (C-1″), 41.2 (C-5″), 43.7 (C-3), 76.4 (C-2), 96.7 (C-6), 103.8 (C-4a), 103.9 (C-3′), 109.5 (C-8), 118.3 (C-1′), 120.9 (C-5′), 124.4 C-10), 124.9 (C-2″), 125.9 (C-7″), 128.9 (C-6′), 131.9 (C-11), 132.5 (C-8″), 136.8 (C-3″), 154.6 (C-2′), 157.1 (C-4′), 162.5 (C-8a), 163.5 (C-5), 166.4 (C-7), 199.3 (C-4).

Neocyclomorusin (**7**)*:* amorphous yellow powder; mp 261−264 °C; $[\alpha]_D$ −0.55 (*c* 0.103, CH_3OH); ^{1}H NMR (500 MHz, $CDCl_3$) δ 7.78 (1H, d, J = 8.8 Hz, H-6′), 6.68 (1H, d, J = 10.0 Hz, H-9), 6.65 (1H, dd, J = 8.8, 2.1 Hz, H-3′), 6.52 (1H, d, J = 2.1 Hz, H-5′), 6.19 (1H, s, H-6), 5.52 (1H, d, J = 10.0 Hz, H-10), 3.96 (1H, dd, J = 9.2, 2.3 Hz, H-2″), 3.22 (1H, dd, J = 16.6, 2.5 Hz, H-1″a), 2.61 (1H, dd, J = 16.6, 9.3 Hz, H-1″b), 1.40 (6H, s, H-12, H-13), 1.30 (3H, s, H-4″), 1.29 (3H, s, H-5″); ^{13}C NMR (125 MHz, $CDCl_3$) δ 25.07 (C-4′), 25.4 (C-1″), 25.9 (C-5″), 28.5 (C-12, C-13), 73.1 (C-3 μ), 78.4 (C-11), 90.9 (C-2 μ), 100.2 (C-6), 101.4 (C-8), 104.4 (C-4a), 108.3 (C-3′), 112.0 (C-5′), 114.7 (C-3), 115.2 (C-9), 116.6 (C-1′), 127.7 (C-10), 130.2 (C-6′), 152.1 (C-8a), 158.7 (C-2), 159.8 (C-7), 160.2 (C-2‘), 161.5 (C-5), 161.8 (C4′), 181.5 (C-4).

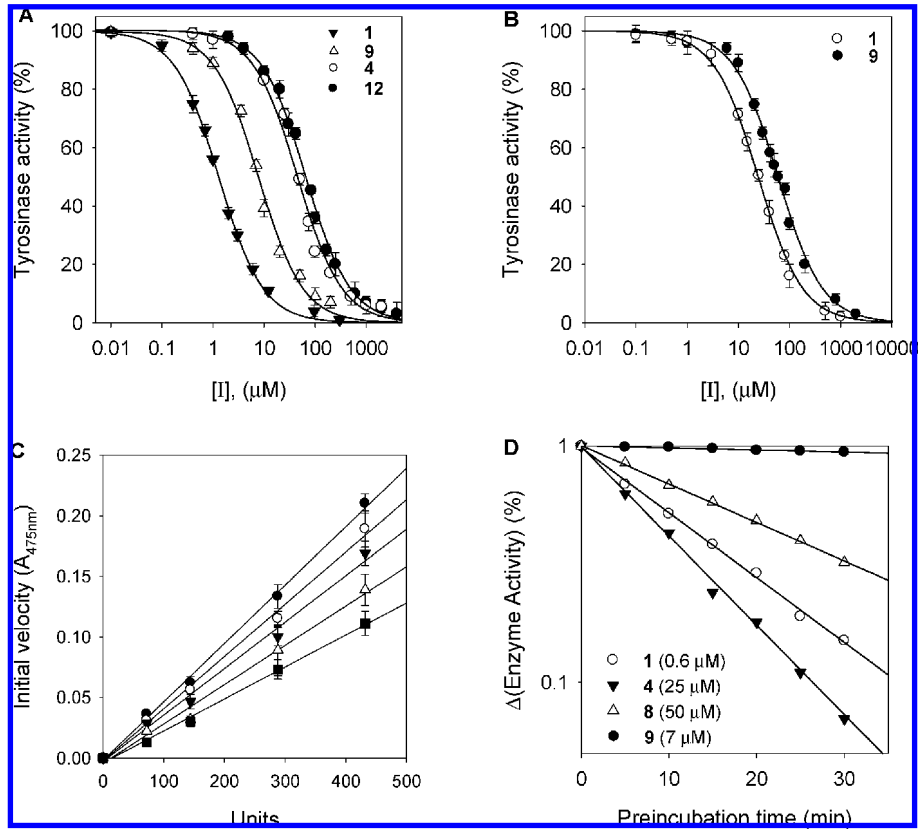

Figure 3. (**A**) Effect of compounds (**1**, **4**, **9**, and **12**) on the activity of tyrosinase for the catalysis of L-tyrosine. (**B**) Effect of compounds **1** and **9** on the activity of tyrosinase for the catalysis of L-DOPA at 30 °C. (**C**) Relationship between the catalytic activity of tyrosinase and concentrations of compound **1**. Concentrations of compound **1** for lines from top to bottom were 0, 0.3, 0.6, 1.0, and 2.0 μM, respectively. (**D**) Inhibition as a function of preincubation time for isolated compounds (**1**, **4**, **8**, and **9**).

Kuwanon A (**8**)*:* amorphous yellow powder; mp 176−177 °C; ^{1}H NMR (500 MHz, acetone-d_6) δ 6.97 (1H, d, J = 8.4 Hz, H-6′), 6.64 (1H, d, J = 10.0 Hz, H-7′), 6.34 (1H, d, J = 8.4 Hz, H-5′), 6.19 (1H, d, J = 2.1 Hz, H-8), 5.61 (1H, d, J = 10.0 Hz, H-8′), 4.97 (1H, m, H-2″), 2.96 (2H, d, J = 7.1 Hz, H-1″), 1.43 (3H, s, H-10′), 1.31 (6H, s, H-12, H-13), 1.26 (3H, s, H-11′); ^{13}C NMR (125 MHz, acetone-d_6) δ 17.5 (C-5″), 25.2 (C-1″), 26.5 (C-4″), 28.2 (C-10′, C-11′), 78.3 (C-9′), 94.7 (C-8), 100.6 (C-6), 104.4 (C-4a), 109.8 (C-5′), 112.6 (C-1′), 115.1 (C-3′), 117.7 (C-7′), 122.6 (C-2″), 130.7 (C-8′), 131.8 (C-6′), 133.8 (C-3″), 152.5 (C-2′), 157.1 (C-4, C-8a), 160.0 (C-3), 161.8 (C-2), 164.9 (C-5), 165.0 (C-7), 184.6 (C-4).

Moracin M (**9**)*:* amorphous yellow powder; mp 261−263 °C; ^{1}H NMR (500 MHz, methanol-d_4) δ 7.24 (1H, d, J = 8.4 Hz, H-4), 6.81 (1H, s, H-4′), 6.80 (1H, d, J = 1.8 Hz, H-7), 6.66 (2H, s, H-2′, H-6′), 6.63 (1H, dd, J = 8.4, 2.1 Hz, H-5), 6.14 (1H, t, J = 4.0, 1.9 Hz, H-4′); ^{13}C NMR (125 MHz, methanol-d_4) δ 98.9 (C-7), 102.6 (C-3), 103.9 (C-4′), 104.4 (C-2′, C-6′), 113.7 (C-5), 122.4 (C-4), 123.5 (C-4a), 134.2 (C-1′), 156.6 (C-2), 157.3 (C-7a), 157.7 (C-6), 160.4 (C-3′27, C-5′).

Moracin N (**10**)*:* yellowish powder; ^{1}H NMR (500 MHz, methanol-d_4) δ 7.09 (1H, s, H-4), 6.79 (1H, s, H-7), 6.76 (1H, s, H-3), 6.65 (1H, s, H-2′), 6.64 (1H, s, H-6′), 6.13 (1H, t, J = 4.3, 2.2 Hz, H-4′), 5.26 (1H, t, J = 2.8, 1.4 Hz, H-9), 3.25 (2H, m, H-8), 1.65 (3H, s, H-11), 1.63 (3H, s, H-12); ^{13}C NMR (125 MHz, methanol-d_4) δ 18.2 (C-11), 26.4 (C-12), 29.9 (C-8), 98.3 (C-7), 102.7 (C-3), 103.8 (C-4′), 104.3 (C-2′, C-6′), 121.8 (C-4), 123.2 (C-4a), 124.8 (C-8), 126.6 (C-6), 133.3 (C-10), 134.4 (C-1′), 155.0 (C-6), 155.9 (C-7a), 156.2 (C-2), 1660.3 (C-3′, C-5′).

Albafuran A (**11**)*:* amorphous yellow powder; mp 131−133 °C; ^{1}H NMR (500 MHz, acetone-d_6) δ 7.08 (1H, d, J = 8.2 Hz, H-4), 6.85 (1H, s, H-3), 6.76 (2H, s, H-7, H-6′), 6.69 (1H, d, J = 8.3 Hz, H-5), 6.24 (1H, s, H-4′), 5.33 (1H, m, H-9), 4.91 (1H, m, H-14), 3.53 (2H, d, J = 7.3 Hz, H-8), 1.95 (2H, m, H-13), 1.86 (2H, m, H-12), 1.77 (3H, s, H-11), 1.42 (3H, s, H-16), 1.37 (3H, s, H-17); ^{13}C NMR (125 MHz, acetone-d_6) δ 16.9 (C-11), 18.1 (C-16), 23.8 (C-8), 26.2 (C-17), 29.8 (C-13), 40.9 (C-12), 103.0 (C-3), 103.9 (C-4′), 104.3 (C-7, C-6′), 112.6 (C-4a), 113.6 (C-5), 119.3 (C-4), 123.0 (C-2′), 123.5 (C-9), 125.5 (C-14), 132.1 (C-15), 134.1 (C-1′), 136.1 (C-10), 153.9 (C-6), 155.8 (C-7a), 155.9 (C-2), 160.2 (C-3′, C-5′).

Moracinoside M (**12**)*:* amorphous white powder; mp 175−(decomp) °C; $[\alpha]_D$ −7.0 (*c* 0.291, CH_3OH); HREIMS *m*/*z* 458.1576 (calcd for $C_{24}H_{26}O_9$, 458.1577); ^{1}H NMR (500 MHz, acetone-d_6) δ 7.11 (1H, s, H-4), 6.90 (1H, s, H-3), 6.90 (1H, s, H-6′), 6.89 (1H, s, H-4′), 6.74 (1H, s, H-7), 6.45 (1H, s, H-2′), 3.69 (1H, dd, J = 7.8, 5.5 Hz, H-2″), 2.96 (1H, d, J = 16.3, 5.3 Hz, H-1″a), 2.70 (1H, dd, J = 16.2, 8.1 Hz, H-1″b), 1.23 (3H, s, H-4″), 1.12 (3H, s, H-5″); xylopyranoside 4.87 (1H, d, J = 6.4 Hz, xyl-H1), 3.82 (1H, dd, J = 11.3, 4.9 Hz, xyl-H5$_\beta$), 3.51 (1H, br m, xyl-H4), 3.39−3.45 (2H, m, xyl-H2 and xyl-H3), 3.32 (1H, t, J = 10.5 Hz, xyl-H5$_\alpha$); ^{13}C NMR (125 MHz, acetone-d_6) δ 21.1 (C-4″), 26.6 (C-5″), 32.8 (C-1″), 70.4 (C-2″), 78.5 (C-3″), 99.8 (C-7), 102.8 (C-3), 105.3 (C-2′), 105.7 (C-4′), 106.7 (C-6′), 118.4 (C-5), 122.2 (C-4), 123.9 (C-4a), 133.7 (C-1′), 153.0 (C-6), 155.8 (C-7a), 155.9 (C-2), 160.1 (C-3′), 160.6 (C-5′); xylopyranoside 66.8 (xyl-C5), 71.1 (xyl-C4), 74.8 (xyl-C3), 77.9 (xyl-C2), 102.9 (xyl-C1). Compound **12** named "moracinoside M" proved to be a new phenylbenzofuran. Our detailed kinetic analysis unveiled that the kinetic modes of these inhibitors were significantly affected by their parent skeletons.

Tyrosinase Assays. Mushroom tyrosinase (EC 1.14.18.1) (Sigma Chemical Co.) was used as described (*9*, *11*) previously with some modifications, using either, L-DOPA (diphenolase) or L-tyrosine (monophenolase) as substrate. In spectrophotometric experiments, enzyme activity was initial velocity (v_i) monitored by observing dopachrome formation at 475 nm with a UV−vis spectrophotometer (Spectro UV−vis double beam; UVD-3500, Labomed, Inc.) at 30 °C. All samples were first dissolved in EtOH at 10 mM. First, 200 μL of a 2.7 mM L-tyrosine (K_m = 180 μM) or 5.4 mM L-DOPA (K_m = 360 μM) aqueous solution was mixed with 2687 μL of 0.25 M phosphate buffer (pH 6.8). Then, 100 μL of the sample solution and 13 μL of the same phosphate buffer solution containing mushroom tyrosinase (144 units) were added in this order to the mixture. Each assay was conducted

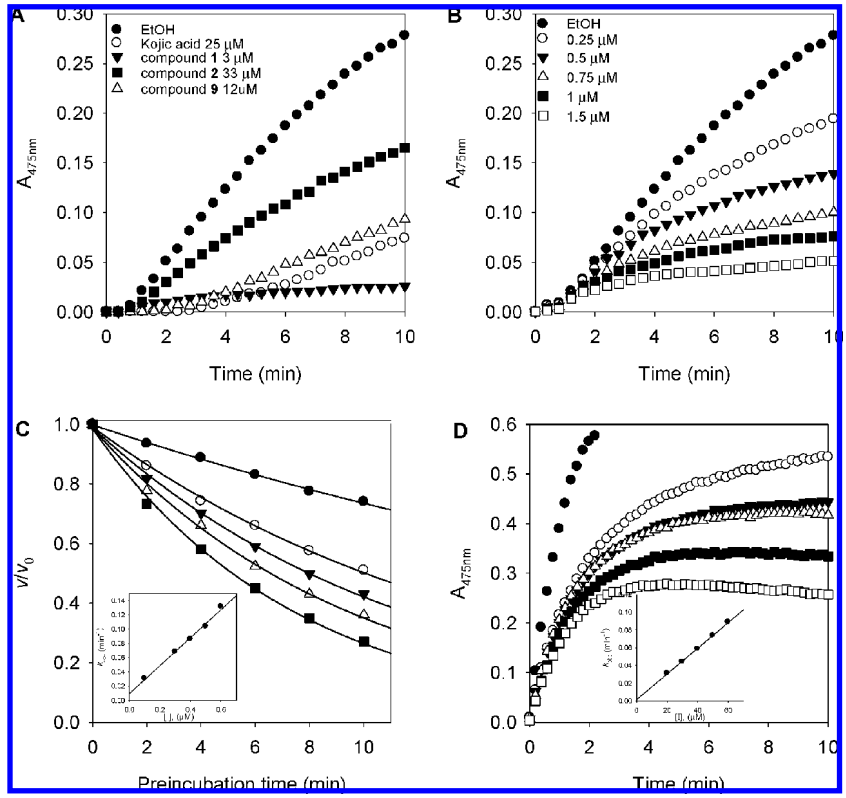

Figure 4. Time course of oxidation of L-tyrosine catalyzed by mushroom tyrosinase in the presence of compounds (**1**, **2**, **9**, and kojic acid). (**A**) Concentrations of compounds **1**, **2**, **9**, and kojic acid were 3 μM, 33 μM, 12 μM, and 25 μM. (**B**) Time-dependent inhibition of tyrosinase in the presence of steppogenin (**1**). Conditions were as follows: 180 μM L-tyrosine, 80 units of tyrosinase, and concentrations of steppogenin for curves from top to bottom were 0, 0.25, 0.5, 0.75, 1.0, and 1.5 μM. (**C**) Time course of the inactivation of tyrosinase by steppogenin. The k_{obs} values at each inhibition concentration were determined by fitting the data to eq 2. (Inset) Dependence of the values for k_{obs} on the concentration of steppogenin by fitting the data to eq 3. (**D**) Time-dependent inhibition of tyrosinase in the presence of steppogenin under the L-DOPA substrate (for curves from top to bottom were 0, 20, 40, 60,100, and 200 μM, respectively).

as three separate replicates. The inhibitor concentration leading to 50% activity loss (IC_{50}) was obtained by fitting experimental data to the logistic curve by eq 1 (*24*):

$$\text{activity (\%)} = 100[1/(1 + ([I]/IC_{50}))] \quad (1)$$

Time-Dependent Assays and Progress Curves. Time-dependent assays and progress curves were carried out using 80 units of tyrosinase, and L-tyrosine and L-DOPA were used as a substrates (respectively from monophenolase and diphenolase assays) in 0.25 M phosphate buffer (pH 6.8) at 30 °C. Enzyme activities were measured continuously for 10 min on a UV spectrophotometer. To determine the kinetic parameters associated with time dependent inhibition of tyrosinase, progress curves with 20 data points (30 s intervals) were obtained at several inhibitor concentrations using fixed substrate concentrations. The data were analyzed using the a nonlinear regression program [Sigma Plot (SPCC Inc., Chicago, IL)] to give the individual parameters for each curve; v_i (initial velocity), v_s (steady-state velocity), k_{obs} (apparent first-order rate constant for the transition from v_i to v_s), A (absorbance at 475 nm), and K_i^{app} (apparent K_i) according to the following equations *24*−*27*):

$$v/v_0 = \exp(-k_{obs}t) \quad (2)$$

$$k_{obs} = k_4(1 + [I]/K_i^{app}) \quad (3)$$

$$A = v_s t + (v_i\text{-}v_s)[1 - \exp(-k_{obs}t)]/k_{obs} \quad (4)$$

A plot of the natural log of the residual enzyme activity versus preincubation time gave a straight line with a slope of $-k_{obs}$. The values of k_3, k_4, and K_i^{app} were calculated from the plot of the k_{obs} versus concentration of inhibitors according to the method of Morrison and Walsh (*24*−*26*).

RESULTS AND DISCUSSION

The chloroform-soluble fraction of the methanolic extract of *Morus lhou* (S.) Koidz. roots after separation by chromatography yielded eleven flavonoids (**1**−**11**). Compounds **1**−**11** are known compounds and were identified by their spectroscopic data as steppogenin (**1**), kuwanon E (**2**), kuwanon U (**3**), 8-isoprenyl-5′-geranyl-5,7,2′,4′-tetrahydroxy flavanone (**4**), norartocarpetin (**5**), morusinol (**6**), neocyclomorusin (**7**), kuwanon A (**8**), moracin M (**9**), moracin N (**10**), albafuran A (**11**). Activity guided fractionation of the methanolic extract also gave moracinoside M (**12**) which was purified over octadecyl-functionalized silica gel. The structural elucidation of new compound is detailed below.

Compound **12** had the molecular formula $C_{24}H_{26}O_9$ and twelve degrees of unsaturation, as deduced from HREIMS (*m*/*z* 458.1576 [M^+]) data. The UV spectrum resembled this of 2-phenylbenzofuran derivatives (*28*). The ^1H and ^{13}C NMR data including DEPT experiments showed the presence of twenty-four carbon atoms: two methylens (sp^3), six methins (sp^2), five methins (sp^3), two methyls, and nine quaternary carbons. The ^{13}C NMR data enabled carbons corresponding to seven aromatic C−C double bonds to be identified, thus accounting for seven of twelve degrees of unsaturation. The remaining five degrees of unsaturation were ascribed to cyclic systems (including the benzofuran ring).

The presence of an epoxyprenyl group was deduced from the connectivity between methylene protons H-1″ (δ_H 2.96, 2.70) and methane proton H-2″ (δ_H 3.67) in the COSY spectrum and correlation of H-2″ with three carbons, C-3″ (δ_C 78.5), 4″ (δ_C

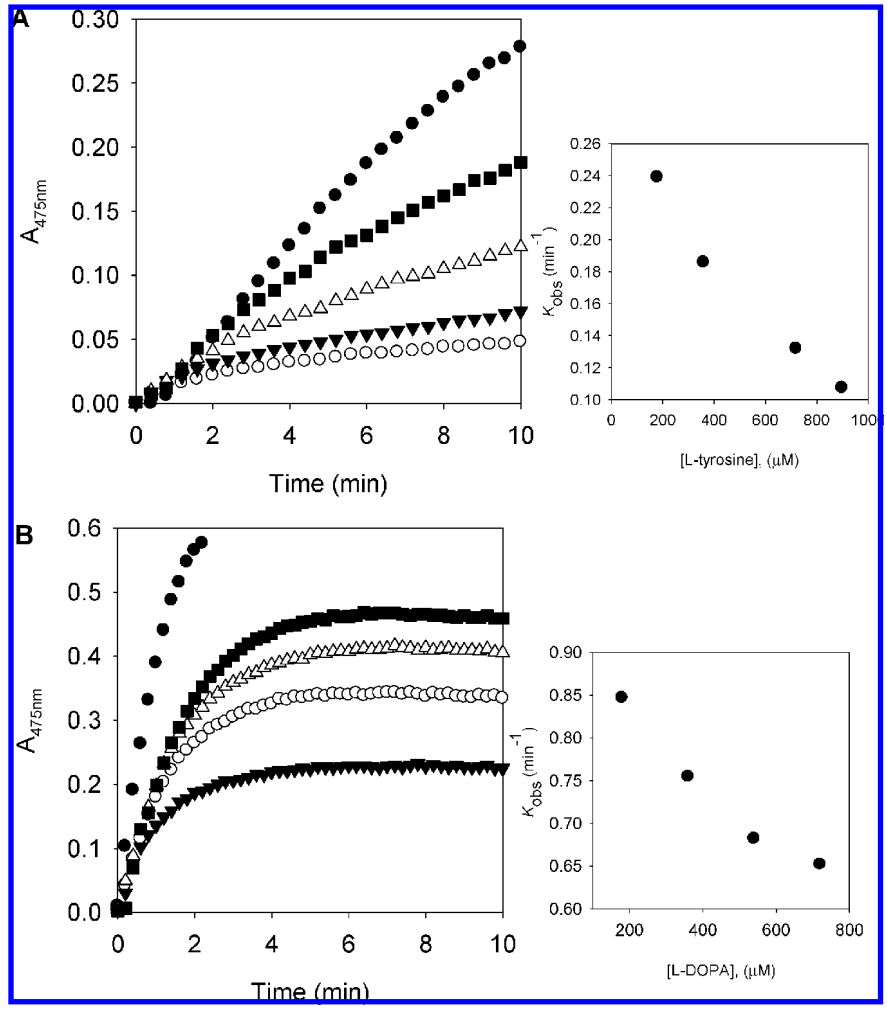

Figure 5. (**A**) Progress curves for the competitive behavior of steppogenin. Conditions were as follows: 1.0 μM steppogenin, 80 units of tyrosinase, and concentration of L-tyrosine for curves from top to bottom were 0, 900, 700, 360, and 180 μM. (Inset) Dependence of the values for k_{obs} on the concentration of L-tyrosine. (**B**) Progress curves for the competitive behavior of steppogenin using L-DOPA as substrate. Conditions were as follows: 100 μM steppogenin, 80 units tyrosinase, and concentration of L-DOPA for curves from top to bottom were 0, 900, 700, 360, and 180 μM. (Inset) Dependence of the values for k_{obs} on the concentration of L-DOPA.

21.0), 5″ (δ_C 26.6) in the HMBC spectrum. The two isolated protons of H-4 and H-7 in the A-ring were observed at 7.11 and 6.74 ppm. The H-3 furan proton in the C-ring occurred at 6.90 ppm with same chemical shift value with H-6′ in the B-ring. Thus, H-2′ and H-4′ appeared at 6.44 ppm and 6.88 ppm as singlet (absence of meta coupling). The abovementioned epoxyprenyl group was placed at C-5 on the A-ring due to HMBC correlation of C-5 with H-1″ and H- 2″ (**Figure 2**). The ^{1}H NMR spectrum exhibited a doublet at δ_H 4.87 (J = 6.4 Hz) indicating the presence of an anomeric carbon which constituted the starting point of COSY analysis. The assignment of pyran structure was determined on the basis of successive connectivities from xyl-1 to xyl-5. In 2D-NOESY experiments in the xylose, an NOE cross peak was observed between *syn*-1,3-diaxial protons xyl-H5$_\alpha$ and xyl-H1 (anomeric proton), whereas xyl-H4 only showed a cross peak with xyl-H5$_\beta$ (**Figure 2**). As we anticipated, there are no NOE cross peaks between xyl-1, xyl-2, xyl-3 and xyl-4, which all have a *trans* diaxial relationship between each other. The *cis* relationship between xyl-H4 and xyl-H5$_\beta$ is also confirmed by the J value of the double doublet corresponding to xyl-H5$_\beta$ [J_1 = 11.0 Hz (germinal), J_2 = 5.0 Hz (vicinal)]. The relative stereochemistry of xyl-H1 and xyl-H2 was easily confirmed by the J value of anomeric proton (δ_H 4.87, J = 6.4 Hz) that is a characteristic of β-xylopyranosyl moiety (*29*, *30*). Acid hydrolysis of **12** yields β-D-xylose a result that was ascertained by GC/MS analysis with reference to an authentic sample. The xylopyranosyl moiety was placed at C-3′ of the B-ring by HMBC. Thus, compound **12** was identified as 5′-[2,3-epoxy-3-methylbutyl]-3′-O-β-D-xylopyranosyl-6,5′-dihydroxy-2-phenylbenzyfuran called moracinoside M.

As shown in **Table 1**, all polyphenols investigated apart from compounds **3** and **6** exhibited a significant (dose-dependent) degree of monophenolase (L-tyrosine substrate) inhibition [(IC_{50} 1.2−160.3 μM) (**Figure 3A**)]. As the concentrations of the inhibitors increased, the residual enzyme activity rapidly diminished. Compounds **1**, **2**, **4**, **5**, **9**, **11**, and **12** emerged to be the most potent inhibitors to monophenolase activity, with IC_{50}s values 1.3, 47.5, 44.2, 1.2, 7.4, 98.5, and 82.5 μM, respectively. It seems that alkyl substitution on any position of the aromatic rings within the parent compounds (**1**, **5**, and **9**) reduces the potency of the inhibitors greatly. The markedly low potency of compound **3** relative to compound **1** suggests that free hydroxyl functions are also paramount to inhibitor activity. As we were interested in each step of the oxidation process, we proceeded to investigate the inhibition of diphenolase activity by these compounds. Interestingly, only two of these compounds, flavanone (**1**) and phenylbenzofuran (**9**), displayed significant inhibitory activities against diphenolse with IC_{50}s of 26.5 and 64.6 μM, respectively (**Figure 3B**). It is noteworthy that these

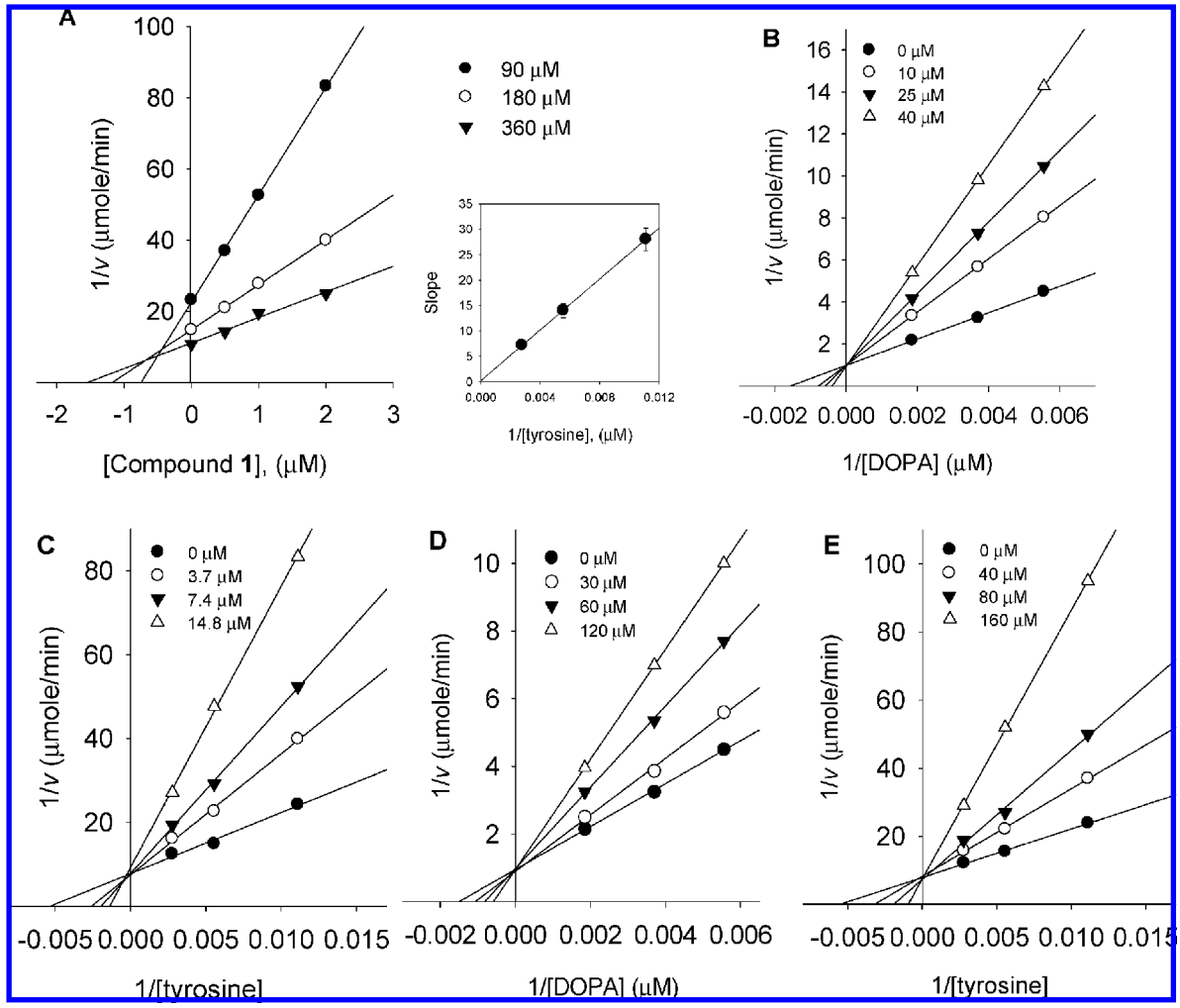

Figure 6. (**A**) Dixon plots for the inhibition of compound **1** on the monophenolase activity of tyrosinase. (Inset) Replot of slope versus the corresponding 1/[S] of compound **1**. In the presence of different concentrations of substrate for lines from bottom to top: 360, 180, and 90 μM. (**B**) and (**D**) Lineweaver−Burk plots for the inhibition of compounds **1** and **9** on the diphenolase activity of tyrosinase. (**C**) and (**E**) Lineweaver−Burk plots for the inhibition of compounds **9** and **12** on the monophenolase activity of tyrosinase. Conditions were as follows: 180 μM L-tyrosine, 360 μM L-DOPA, 144 units of tyrosinase, 0.25 M phosphate buffer (pH 6.8), at 30 °C. In the presence of different concentrations of compounds for lines from bottom to top: (**B**) for compound **1**, 0, 10, 25, and 40 μM; (**C**) for compound **9**, 0, 3.7, 7.4, and 14.8 μM; (**D**) for compound **9**, 0, 30, 60, and 120 μM; (**E**) for compound **12**, 0, 40, 80, and 160 μM.

values are more than 20-fold greater than the corresponding IC_{50}s for monophenolase.

The inhibition mechanisms displayed by the isolated polyphenols were subsequently studied. All inhibitors manifested the same relationship between enzyme activity and enzyme concentration. The inhibition of mushroom tyrosinase by compound **1** is illustrated in **Figure 3C** representatively. Plots of the initial velocity versus enzyme concentration in the presence of different concentrations of steppogenin (**1**) gave a family of straight lines, all of which passed through the origin. Increasing the inhibitor concentration resulted in a lowering of the line gradients, indicating that these compounds were reversible inhibitors. To investigate the enzyme activity as a function of time exposed to the inhibitor, we measured residual enzyme activity of preincubated enzyme with inhibitors over a number of exposure times. Flavanones (**1** and **4**) and flavone (**8**) showed a time-dependent inhibitory effect on tyrosinase activity, whereas phenylbenzofuran (**9**) did not. In our previous work, it was proven that flavone (**5**) showed a time-dependent inhibitory effect (*11*).

We then undertook the full kinetic characterization of these inhibitors. **Figure 4A** depicts the time course for the oxidation of L-tyrosine catalyzed by tyrosinase in the presence of compounds **1**, **2**, **9**, and kojic acid. As expected, in the presence of monophenolase inhibitors, the lag time was prolonged from 60 s in the control to 210 s with addition of inhibitors. Also, the lag time of positive control was 210 s at 25 μM. Compound **9** emerged not to be a time-dependent inhibitor whereas the other inhibitors (**1** and **2**) showed time-dependent inhibition profiles (**Figure 4A**). These results echo the preincubation experiments (**Figure 3D**). The potent tyrosinase inhibitor, flavanone (**1**), showed a typical progress curve for slow-binding inhibition at low concentrations. Slow-binding inhibition mechanisms can be investigated by preincubation of the enzyme with inhibitor followed by measurement of initial velocities for substrate oxidation as a function of preincubation time. Increasing flavanone (**1**) concentration led to a decrease in both the initial velocity (v_i) and the steady-state rate (v_s) (**Figure 4B**). The progress curves obtained using various concentrations of the inhibitors were fitted to eq 2 to determine v_i, v_s, and k_{obs}. The k_{obs} values were plotted as a function of steppogenin concentration. The results indicated that steppogenin inhibits mushroom tyrosinase by simple reversible slow binding when L-tyrosine was used as a substrate (**Figure 4C**). This was backed

up by the observation that the k_{obs} values exhibited a linear dependence on the inhibitor concentration as shown in **Figure 4C** inset. Also, **Figure 4D** showed typical progress curves for slow binding behavior, when the oxidation of L-DOPA was catalyzed by mushroom tyrosinase in the presence of different steppogenin concentrations. Thus, analysis of data according to eqs 2 and 3 yielded the following values: $k_3 = 0.196605$ min^{-1} μM^{-1}, $k_4 = 0.009209$ min^{-1}, $K_i^{app} = 0.04684$ μM. Steppogenin also emerged as a simple reversible slow-binding inhibitor of diphenolase ($k_3 = 0.001445$ min^{-1} μM^{-1}, $k_4 = 0.0013$ min^{-1}, $K_i^{app} = 0.8996$ μM). Similar kinetic analysis previously reported from our group delineated that flavone **5** effected slow-binding enzyme isomerization. Thus, despite having similar molecular size and functionality, and almost equal inhibitory potencies toward monophenolase, steppogenin inhibits both monophenolase and diphenolase via the simple reversible slow-binding mode whereas flavone (**5**) was active only against monophenolase through enzyme isomerization (*11*).

Most slow-binding enzyme inhibitors act as competitive inhibitors, binding at the enzyme active site (*24*, *26*), although it is possible for them to interact with the enzyme by competitive, noncompetitive, or uncompetitive inhibition patterns. To distinguish the mode of inhibition of a time-dependent inhibitor, it is convenient to analyze the effect of various substrate concentrations of k_{obs} at fixed inhibitor concentration. A competitive inhibitor will display a decrease of k_{obs} with increasing substrate concentrations, while for a noncompetitive inhibitor the value of k_{obs} is independent of substrate concentrations. **Figure 5A** illustrates typical progress curves of time-dependent inhibition of steppogenin (1.0 μM) when the enzymatic reaction is initiated by the addition of tyrosinase (80 units), in the presence of various concentrations of L-tyrosine (180, 360, 700, and 900 μM). The k_{obs} values were determined by fitting data to eq 4. As a result, steppogenin is a competitive inhibitor because k_{obs} decreased with increasing substrate concentration (inset). When L-DOPA was used as a substrate, steppogenin also exhibited competitive inhibition (**Figure 5B**). Recently, many researchers reported that resorcinol can be classified as slow-binding competitive inhibitor of mushroom tyrosinase. Consistent with the structural similarities to the inhibitors employed in the above results, our inhibitors also show time dependent inhibition behavior.

Finally, we investigated the characteristics of inhibitors **1**, **9**, and **12** with respect to the two different steps carried out by the enzyme individually. In this experiment, the initial velocity of the enzyme was monitored by observing dopachrome formation at 475 nm. Compound **1** displayed competitive inhibition against both monophenolase ($K_i = 0.7$ μM) and diphenoalse ($K_i = 14.1$ μM) as shown in Dixon (**Figure 6A**) and Lineweaver−Burk plots (**Figure 6B**) respectively. Phenylbenzofuran (**9**) showed competitive inhibition against both monophenolase ($K_i = 4.4$ μM) and diphenolase ($K_i = 64.6$ μM) by Lineweaver−Burk plots. The new compound **12** also showed competitive inhibition [($K_i = 33.4$ μM) Lineweaver−Burk plot]. Most competitive inhibitors of tyrosinase bind to the active site mimicking the enzyme/substrate interaction. The B-ring of our isolated compounds is very similar to tyrosinase substrates (tyrosine and DOPA). This leads to the competitive displacement of substrates from the active site of the cofactor in a lock-and-key model. Some flavonoids have been described to chelate copper (*7*) which has been suggested as a mode of inhibition. However, no shift in the UV−visible spectra was observed by adding Cu^{2+} to these species.

In conclusion, twelve polyphenols were successfully isolated and purified from *M. lhou* including a new phenylbenzofuran (**12**), which we named "moracinoside M". The inhibitory potencies and capacities of these flavonoids toward the monophenolase activity of mushroom tyrosinase were studied in detail. Interestingly, they showed different inhibitory modes depending upon the skeleton: simple reversible slow-binding (time dependent) for flavanones, enzyme isomerization for flavones, and a simple competitive inhibition for phenylbenzofurans (time independent). The enzymatic oxidation of tyrosine to melanin is of considerable importance since melanin has many important functions and alterations in melanin synthesis occur in many diseases. The flavonoid-derived tyrosine inhibitors studied herein displayed the most potent inhibition profiles suggesting that they are excellent candidates to be developed as effective antibrowning agents for foodstuff of skin whitening agents in cosmetics.

ABBREVIATIONS USED

IC_{50}, the inhibitor concentration leading to 50% activity loss; K_i, inhibition constant; K_i^{app}, apparent K_i; k, rate constant; V_{max}, maximum velocity; K_m, Michaelis−Menten constant; k_{obs}, apparent first-order rate constant for the transition from v_i to v_s; v_i, initial velocity; v_s steady-state rate; A, absorbance at 475 nm.

LITERATURE CITED

(1) Fu, B.; Li, H.; Wang, X.; Lee, F. S. C.; Cui, S. Isolation and identification of flavonoids in licorice and a study of their inhibitory effects on tyrosinase. *J. Agric. Food Chem.* **2005**, *53*, 7408–7414.

(2) Meada, K.; Fukuda, M. J. In vitro effectiveness of several whitening cosmetic components in human melanocytes. *Soc. Cosmet. Chem.* **1991**, *42*, 361–368.

(3) Mcevily, J. A.; Iyengar, R.; Otwell, Q. S. Inhibition of enzymatic browning in food and beverages. *Crit. Rev. Food Sci. Nutr.* **1992**, *32*, 253–273.

(4) Halaouli, S.; Asther, M.; Sigoillot, J. C.; Hamdi, M.; Lomascolo, A. Fungal tyrosinases: New prospects in molecular characteristics, bioengineering and biotechnological applications. *J. Appl. Microbiol.* **2006**, *100*, 219–232.

(5) Mayer, A. M. Polyphenol oxidases in plants and fungi: Going places? A review. *Phytochemistry* **2006**, *67*, 2318–2331.

(6) Fenoll, L. G.; Penalver, M. J.; Rodriguez-Lopez, J. N.; Varon, R.; Garcia-Canovas, F.; Tudela, J. Tyrosinase kinetics: Discrimination between two models to explain the oxidation mechanism of monophenolase and diphenolase substrates. *Int. J. Biochem. Cell Biol.* **2004**, *36*, 235–246.

(7) Kubo, I.; Nihei, K. I.; Shimizu, K. Oxidation products of quercetin catalyzed by mushroom tyrosinase. *Bioorg. Med. Chem.* **2004**, *12*, 5343–5347.

(8) Matsuura, R.; Ukeda, H.; Sawamura, M. Tyrosinase inhibitory activity of citrus essential oils. *J. Agric. Food Chem.* **2006**, *54*, 2309–2313.

(9) Kubo, I.; Kinst-Hori, I. Tyrosinase inhibitors from cumin. *J. Agric. Food Chem.* **1998**, *46*, 5338–5341.

(10) Shimizu, K.; Kondo, R.; Sakai, K. Inhibition of tyrosinase by flavonoids, stilbenes and related 4-substuted resorcinols: Structure-activity investigations. *Planta Med.* **2000**, *66*, 11–15.

(11) Ryu, Y. B.; Ha, T. J.; Curtis-Long, M. J.; Ryu, H. W.; Gal, S. W.; Park, K. H. Inhibitory effects on mushroom tyrosinase by flavones from the stem barks of *Morus lhou* (S.) Koidz. *J. Enzyme Inhib. Med. Chem.* **2008**, *23*, 922–930.

(12) Singab, A. N. B.; El-Beshbishy, H. A.; Yonekawa, M.; Nomura, T.; Fukai, T. Hypoglycemic effect of Egyptian *Morus alba* root bark extract: Effect on diabetes and lipid peroxidation of streptozotocin-induced diabetic rats. *J. Ethnopharmacol.* **2005**, *100*, 333–338.

(13) Du, J.; He, Z. D.; Jiang, R. W.; Ye, W. C.; Xu, H. X.; But, P. P. X. Antiviral flavonoids from the root bark of *Morusalba* L. *Phytochemistry* **2003**, *62*, 1235–1238.
(14) Fukai, T.; Satoh, K.; Nomura, T.; Sakagami, H. Antinephritis and radical scavenging activity of prenylflavaonoids. *Fitoterapia* **2003**, *74*, 720–724.
(15) Li, H.; Cheng, K.-W.; Cho, C.-H.; He, Z.; Wang, M. Oxyresveratrol as an antibrowning agent for cloudy apple juices and fresh-cut apples. *J. Agric. Food Chem.* **2007**, *55*, 2604–2010.
(16) Lee, S. H.; Choi, S. Y.; Kim, H.; Hwang, J. S.; Lee, B. G.; Gao, J. J.; Kim, S. Y. Mulberroside F isolated from the leaves of *Morus alba* inhibits melanin biosynthesis. *Biol. Pharm. Bull.* **2002**, *25*, 1045–1048.
(17) Nomura, T.; Fukai, T.; Kuwanon, E. a new flavones derivatives from the root bark of the cultivated mulberry tree. *Heterocycles* **1978**, *9*, 1295–1300.
(18) Ferari, F.; Monacelli, B.; Messana, I. Comparison between in vivo and in vitro metabolite production of *Morus nigra*. *Planta Med.* **1999**, *65*, 85–87.
(19) Yamaguchi, T.; Sato, S.; Mihashi, H.; Nomura, T. Aldose reductase inhibitors containing benzypyrans for treatment of diseases associated with diabetes. *Jpn. Kokai Tokkyo Koho* **1999**, 9.
(20) Nomura, T.; Fukai, T.; Katayanagi, M. Studies on the constituents of the cultivated mulberry tree. III Isolation of four new flavones, kuwanon A, B, C and oxydihydromorusin from the root bark of *Morus alba L.* *Chem. Pharm. Bull.* **1978**, *26*, 1453–1458.
(21) Nomura, T.; Fukai, T.; Yamada, S.; Katayanagi, M. Phenolic constituents of the cultivated mulberry tree (*Morus alba L.*). *Chem. Pharm. Bull.* **1976**, *24*, 2898–2900.
(22) Purusotam, B.; Shigetoshi, K.; Satoshi, T.; Mineo, S.; Tsuneo, N. Two new 2-arylbenzofuran derivatives from hypoglycemic activity-bearing fractions of *Morus insigmis*. *Chem. Pharm. Bull.* **1993**, *41*, 1238–1243.
(23) Takasugi, M.; Ishikawa, S.-I.; Masamune, T. Albafurans A and B, geranyl 2-phenylbenzofurans from mulberry. *Chem. Lett.* **1982**, *8*, 1221–1222.
(24) Copeland, R. A. *Enzyme: A practical introduction to structure, mechanism, and data analysis*; Wiley-VCH: New York, 2000; pp 266−332.
(25) Frieden, C. Kinetic aspects of regulation of metabolic processes. The hyseretic enzyme concept. *J. Biol. Chem.* **1970**, *245*, 5578–5799.
(26) Morrison, J. F.; Walsh, C. T. The behavior and significance of slow-binding enzyme inhibitors. *Adv. Enzymol. Relat. Areas Mol. Biol.* **1988**, *61*, 201–301.
(27) Sculley, M. J.; Morrison, J. F.; Cleland, W. W. Slow-binding inhibition: The general case. *Biochim. Biophys. Acta-Protein Struct. Mol. Enzymol.* **1996**, *1298*, 78–86.
(28) Scott, A. I. *Interpretation of the ultraviolet spectra of natural product*; Pergamon Press: London, 1964.
(29) Aquino, R.; Morelli, S.; Lauro, M. R.; Abdo, S.; Saija, A.; Tomaino, A. Phenolic constituents and antioxidant activity of an extract of *Anthurium versicolor* leaves. *J. Nat. Prod.* **2001**, *64*, 1019–1023.
(30) De Tommasi, N.; Piacente, S.; Gacs-Baitz, E.; De simone, F.; Pizza, C.; Aquino, R. Triterpenoid saponins from *Spergularia ramose*. *J. Nat. Prod.* **1998**, *61*, 323–327.

Received for review August 27, 2008. Revised manuscript received December 14, 2008. Accepted December 14, 2008. This study was supported by a grant of the Korea Healthcare technology R&D Project, Ministry of Health & Welfare (A080813), the MOST/KOSEF to the Environmental Biotechnology National Core Research Center (R15-2003-012-0200-0), and the MEST/KOSEF (Nuclear R&D Program, 2007-00614), Republic of Korea.

JF8033286